Neuron, Vol. 41, 181–184, January 22, 2004, Copyright ©2004 by Cell Press

Frisking the Whiskers: Patterned Sensory Input in the Rat Vibrissa System

Minireview

Samar B. Mehta[1] and David Kleinfeld[1,2,3,*]
[1]Graduate Program in Neurosciences
[2]Department of Physics
[3]Center for Theoretical Biological Physics
University of California, San Diego
La Jolla, California 92093

How are two prominent environmental features, surface texture and object location, transduced and encoded as rats whisk? Recent papers show that textures may excite intrinsic mechanical vibrations of the vibrissae. Although these vibrations are too rapid to be directly followed by cortical neurons, there is evidence that their speed is encoded by contact-dependent sensory signals. In addition to contact, sensory signals exist that report the angular position of the vibrissae. The combination of contact and reference signals may be used to decode spatial variations in the environment, particularly the location of objects in head-centered coordinates.

The remarkable organization of vibrissa areas in the rodent nervous system has made it a popular test bed for neurobiological study. In particular, the large, discrete representation of the vibrissa sensorimotor organs in cortex emphasizes the ethological weight carried by the vibrissae on a rodent's cheeks. Schiffman et al. (1970) asked if the tactile perceptions carried by these long hairs can, in fact, dominate the world view of the rat. They made use of a visual cliff, constructed with a platform raised a variable height above a sheet of glass, to give conflicting visual and tactile information about the depth of the underlying floor. On one side of the platform, a checkerboard patterned floor lay immediately underneath the glass, while on the opposite side the same floor pattern was approximately half a meter below the glass and gave the visual impression of a drop. When the platform is raised so that rats cannot touch the glass without jumping, they show a strong preference to descend to the seemingly shallower side. However, when the platform is low enough for the rats to touch the glass with their vibrissae, the preference is lost and the rats readily descend to the seemingly deep side. Thus, vibrissa cues can dominate visual input in rat.

Unfortunately, most early efforts to characterize the function of the vibrissae did not yield results as unequivocal as those of Schiffman et al. (1970). Vincent (1912) used animals that lacked either eyesight, vibrissa somatosensation, or both and examined their performance on tests of locomotion and the use of tactile cues in maze running. Vincent found that only when deprived of both vibrissae and eyesight do rats show severe deficiencies, suggesting that the animals normally use both senses to navigate. In a review of behavioral research performed up to the mid 1970s, Gustafson and Felbain-Keramidas (1977) summarized a variety of complex behaviors, ranging from aggression to swimming, that are affected by the loss of the vibrissae. However, as they point out, behavioral plasticity in the use of other senses can obscure an understanding of precisely which environmental variables are encoded by the vibrissae.

Hutson and Masterton (1986) answered the need for sensory tests designed to isolate perceptual functions of the vibrissae and found that blind rats with intact vibrissae will leap across wider gaps than those without vibrissae. Thus, the vibrissae allow animals to make a binary determination of the existence of the far side of a gap. A similar binary role for the vibrissae, but not the short hairs, follows from studies on the detection of differently shaped objects (Brecht et al., 1997). Other experiments revealed that, far from simply serving as contact detectors, the vibrissae can be used to discriminate between spatially extended objects. Guic-Robles et al. (1989) and Carvell and Simons (1990) used a variant of the gap-crossing task to assess the ability of rats to discriminate differences in surface roughness with their vibrissae. Their data revealed that rats discriminate with an acuity that rivals that of the human fingertip.

Texture is not the only fine sense transduced by the vibrissae. Recent experiments suggest that the vibrissae convey sufficient spatial information to allow rats to distinguish between barriers whose distance from the head varies by less than 5% (Krupa et al., 2001) and to distinguish between objects of different shape and texture (Harvey et al., 2001). It remains unclear, however, if rats can decode the location of objects relative to their head as they explore their environment with synchronous, large-amplitude whisks of their vibrissae.

Texture

The essential result from texture discrimination is that rats can distinguish between cylinders with different pitches of corrugations machined across their surface (Carvell and Simons, 1990, 1995; Guic-Robles et al., 1989). How does this occur? One possibility, first discussed by Carvell and Simons (1995) and bolstered by recent results from Fend et al. (2003), Hartmann et al. (2003), and Neimark et al. (2003), is that the mechanical properties of the vibrissae act to translate surface roughness into a spike rate. Vibrissae are slender, tapered beams and, like all beams, their transient mechanical response may be expressed in terms of intrinsic vibration modes. Each mode is described by a pattern of bending of the vibrissa and has a characteristic vibration frequency.

As a vibrissa drags across a surface, we posit that it alternately sticks and slips across rough features, whether the surface is corrugated or irregular. This leads to bending and release of the vibrissa (Figure 1A). As the vibrissa snaps back and subsequently vibrates, the resultant motion of the shaft is a superposition of vibrations at the intrinsic modes of the vibrissa. Differences between surfaces are expressed by the extent to which different modes are favored. This situation is conceptually the same as exciting different modes in a bowed string and was recently demonstrated for the vibrissae (Fend et al., 2003; Neimark et al., 2003). In particular,

*Correspondence: dk@physics.ucsd.edu

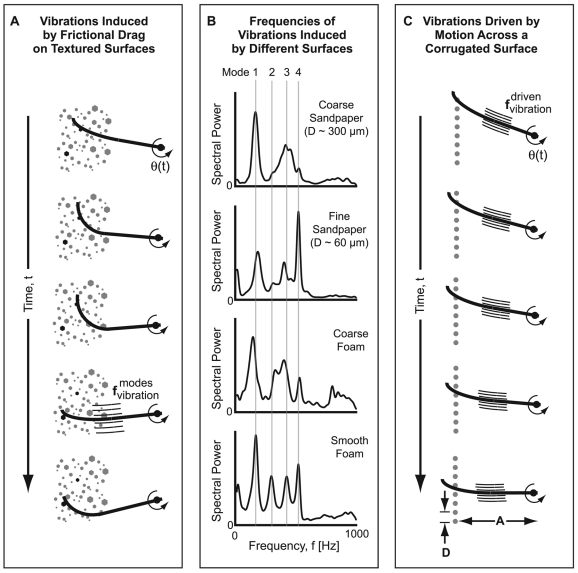

Figure 1. Encoding Texture by Contact of a Vibrissa with a Rough Surface

(A) Cartoon that shows how the drag on a vibrissa can couple to the intrinsic mechanical vibrations (modes) of the vibrissa. (B) Spectral power of the vibrations measured at the base of a vibrissa artificially whisked across different textures. Adapted from Fend et al. (2003). (C) Cartoon that shows how the sweeping motion of a vibrissa across corrugations could induce vibrations in the vibrissa shaft.

Fend et al. (2003) attached the base of a plucked vibrissa to a force transducer and moved the tip of the vibrissa across surfaces of differing roughness. They found that the set of frequencies of the vibration was essentially the same for all surfaces they considered. We associate these frequencies with the intrinsic vibration modes (1 through 4 in Figure 1B; slight shifts in frequency are presumably due to loading) and denote them by $\mathbf{f}^{mode}_{vibration}$. The relative amplitudes of each mode, $\delta\theta^{mode}$, depended on the detailed properties of the surface (Figure 1B). Thus, the angular vibrissa motion, $\delta\theta(t)$, induced by drag across a texture is given by

$$\delta\theta(t) \approx \delta\theta^{(mode\ 1)} sin[2\pi\ \mathbf{f}^{(mode\ 1)}_{vibration} t] + \delta\theta^{(mode\ 2)} sin[2\pi\ \mathbf{f}^{(mode\ 2)}_{vibration} t] + \cdots \quad (1)$$

and encoding of different textures is transformed to encoding the amplitude of motion at the intrinsic frequencies. What evidence supports this encoding by sensory neurons?

The Merkel sensory terminals in vibrissa follicles are capable of tracking vibrations well above 1 kHz (Gottschaldt and Vahle-Hinz, 1981), which encompasses the range of intrinsic frequencies (Figure 1B). Thus, the spiking output of primary sensory neurons in the trigeminal ganglion should be able to lock to the oscillatory motion of the vibrissa. Locking still occurs at the level of the secondary sensory neurons in nucleus principalis, albeit up to slightly lower frequencies (Deschenes et al., 2003). In contrast, the phase-locked response of neurons in vibrissa areas of ventral posterior medial thalamus (Castro-Alamancos, 2002) and primary sensory (S1) cortex (Ahissar et al., 2000; Simons, 1978) are limited to tens of hertz, although it appears that neurons in vibrissa S1 cortex can fire up to hundreds of hertz (Barth, 2003). It is of interest that Arabzadeh et al. (2003) observed that the spike rate of neurons in S1 cortex does not lock to the high-frequency movements of the vibrissae. Rather, the spike rate is of the form Rate $\propto$ *log*$\{\delta\theta^{mode}\ \mathbf{f}^{mode}_{vibration}\}$, where $\delta\theta^{mode}\ \mathbf{f}^{mode}_{vibration}$ corresponds to the maximum speed of vibrissa deflection.

We consider how the observed dependence of the spike rate in cortex may allow the rat to encode texture in terms of the natural frequencies of the vibrissae. Two assumptions are required. First, primary neurons must respond to the velocity of deflection, consistent with observations (Gottschaldt and Vahle-Hinz, 1981). For simplicity, we calculate the velocity for the case of only a single vibration mode, for which the angular velocity induced by drag across a texture is given by

$$\frac{d\{\delta\theta(t)\}}{dt} \approx \delta\theta^{(mode\ 1)}\ \mathbf{f}^{(mode\ 1)}_{vibration} cos[2\pi\ \mathbf{f}^{(mode\ 1)}_{vibration} t]. \quad (2)$$

Second, spiking locked to this fast signal must be demodulated and low-pass filtered along the trigeminal-to-cortical pathway, i.e., the spike rate should depend only on the magnitude of the velocity. For the particular case of demodulation by rectification, e.g., solely excitatory synaptic input, the spike rate is proportional to

$$\text{Spike Rate} \propto function \left\{ \int_{multiple\ cycles} dt \left[\frac{d}{dt} \delta\theta(t) \right]_+ \right\}$$

$$\propto function\ \{\delta\theta^{(mode\ 1)}\ \mathbf{f}^{(mode\ 1)}_{vibration}\} \quad (3)$$

Thus, the spike rate here, as well as for other demodulation schemes, depends directly on the coupling of the vibrissae to the surface. The function that relates the spike rate to the input can be approximately logarithmic (Engel et al., 1999). This interpretation provides the basis for discrimination with only one vibrissa (Fend et al., 2003). In fact, the data confirm that discrimination between pairs of substantially differing textures is not blocked in rats shaved down to a single vibrissa, with the caveat that the case for closely related textures is ambiguous (Carvell and Simons, 1995). It remains an open issue if discrimination across a larger set of textures requires the presence of multiple vibrissae with distinct intrinsic frequencies (Neimark et al., 2003). Further, it is unknown how the spike rate scales for concurrent vibrations at multiple frequencies.

An alternative hypothesis that is applicable to the discrimination of corrugated surfaces is that the frequency of vibrations in the vibrissae is directly induced by surface texture (Figure 1C). To assess this possibility, we estimate the frequency of vibrations in the shaft of a vibrissa from the spacing of the surface features and the parameters of rhythmically driven motion. The angular position of the shaft is described by a single variable, θ. We express the time dependence of θ as a sinusoid with amplitude θ_0 and a center position θ_{set}. Thus,

$$\theta(t) = \theta_{set} + \theta_0 sin[2\pi\ \mathbf{f}_{whisk} t + \phi] \quad (4)$$

where $\mathbf{f}_{whisk}$ is the $\sim$9 Hz frequency of exploratory whisking (Berg and Kleinfeld, 2003) and, in anticipation

of the discussion on contact angle, ϕ is a phase that specifies the origin of time. The frequency of contact of the vibrissa with successive corrugations is greatest, and least variable, near the midpoint of the sweep of vibrissa. Its value, denoted by $f^{driven}_{vibration}$, is estimated as

$$f^{driven}_{vibration} \approx \frac{A}{D} \bullet \left|\frac{d\theta}{dt}\right|_{maximum} = 2\pi \bullet \frac{A}{D} \bullet \theta_0 \, f_{whisk} \qquad (5)$$

where the pitch of the corrugations is given by D, the typical distance from the base of the vibrissa to the contact point is denoted by A, and θ_0 is in units of radians. Using values taken from texture discrimination experiments, e.g., A ~25 mm, D ~15–1000 μm, and θ_0 ~10°–15° (0.17–0.26 radians) (Carvell and Simons, 1995), we find $f^{driven}_{vibration}$ ~300–20,000 Hz. The upper frequencies are too high for even primary sensory neurons to follow. Furthermore, high frequencies preferentially excite the tip, and not the base, of a tapered beam (Cranch and Adler, 1956). Thus, except for the lowest frequencies, which correspond to coarse corrugations, the directly induced vibrations are unlikely to account for the texture discrimination described in the literature.

Location

We now turn to the determination of the position of an external object. The behavioral evidence for involvement of the vibrissae in this task is incomplete, although the studies of Vincent (1912) suggest that rats use their vibrissae to orient toward a point of contact. How could a rat determine where an object is in head-centered coordinates? For the rostral-caudal angle, the issue is that the rat needs to deduce vibrissa position at the time of contact, which is equivalent to determining the phase variable ϕ in Equation 2.

From the perspective of spatial encoding, there are three signals that can be produced in the sensory fibers that innervate the follicle of each vibrissa (Figure 2A). *(1) A reference signal that reports angular position of the vibrissae independent of contact*. Neurons that encode position will preferentially spike at a preferred angle, denoted θ_{Ref}, during the whisking cycle. *(2) A contact-based signal that is generated when a vibrissa first touches an object during protraction*. We refer to this as the ON-contact signal for a given vibrissa. *(3) A contact-based signal that is generated when a vibrissa detaches from an object during retraction*. We refer to this as the OFF-contact signal.

Any two of the above three sensory signals could be used to determine vibrissa angle upon contact. Although there is a lack of evidence for spindle fibers in the facial musculature (Rice et al., 1994), recent results from Szwed et al. (2003) show that reference signals are present in a subset of primary sensory neurons located in the trigeminal nucleus (left panel, Figure 2B). Furthermore, different neurons preferentially spike at different angles during either the protraction or retraction phase of the whisk cycle (right panel, Figure 2B), with a bias toward protraction from the retracted position. These observations made use of a form of fictive whisking in which motion of the vibrissae was induced by rhythmic electrical stimulation of the facial motor nerve (Zucker and Welker, 1969).

The recent results provide a substrate for the observation of a reference signal at the level of vibrissa S1 cortex (Fee et al., 1997). In the latter study, rats were trained to whisk in air, and the reference signal appeared as spikes locked to the rhythmic motion of the vibrissae, as measured via the mystacial electromyogram (left panel,

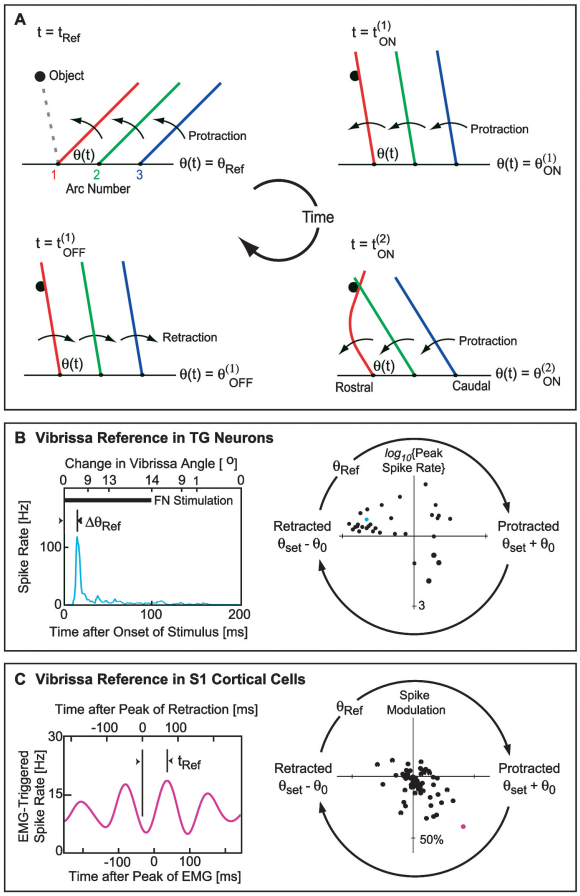

Figure 2. Encoding of Object Location Based on Reference and Contact Spike Signals

(A) Cartoon of a single row of vibrissae at various times relative to their contact with an object. (B) Spiking output from primary sensory neurons of the trigeminal ganglion (TG) was recorded during vibrissa motion induced by 5 Hz electrical stimulation of the facial motor nerve (FN). The left panel shows the trial-averaged response of the reference signal for one neuron; the spiking of this cell was not affected by contact (data not shown). The angle $\Delta\theta_{Ref}$ is the extent of protraction, relative to the initial retracted position, at the peak of the neuronal response. The right panel summarizes the data for all cells with reference responses (Szwed et al., 2003). The radial coordinate is the logarithm of the peak spike rate, and the angular coordinate, θ_{Ref}, is found by $\theta_{Ref} = \Delta\theta_{Ref} - (\theta_{set} - \theta_0)$ where $2\theta_0$ is the maximum defection of the vibrissa, e.g., 14° for the data on the left. (C) Responses in vibrissa S1 cortex measured as animals whisked without contact. The data on the left shows an example of the correlation between spiking and the peak of the electromyogram (EMG). The scale on top accounts for the 25 ms lag between vibrissa position and the EMG (Berg and Kleinfeld, 2003) and the half-period, i.e., 58 ms for this data, between protraction and retraction. The time t_{Ref} is the peak of cortical spiking relative to the fully retracted position. The panel on the right summarizes the data for all cells (Fee et al., 1997); note that the summary plot in the original paper was inverted ($\theta \leftarrow -\theta$). The radial coordinate is the percent depth of modulation of the spike-EMG correlation, and the angular coordinate, θ_{Ref}, is found by $\theta_{Ref} = \theta_{set} - \theta_0 cos\{2\pi\, f_{whisk} t_{Ref}\}$.

Figure 2C). As in the case of primary sensory cells, different neurons were found to have different preferred angles along the whisk cycle (right panel, Figure 2C) and were observed to spike over the full-whisking cycle. However, the distribution of spiking for cells in S1 cortex was biased toward retraction from the protracted position, as opposed to protraction from the retracted position for the case of primary sensory neurons activated by fictive whisking (cf. right panels in Figures 2C and 2D). This difference may result in part from the active nature of retraction in normal whisking (Berg and Kleinfeld, 2003).

The experimental data on the responses of primary sensory neurons (Szwed et al., 2003) show that both reference and ON- and OFF-contact signals are available to deduce contact angle in head-centered coordinates. We consider the simplest decoding scheme, which uses reference and ON-contact signals (Figure 2A). The probability of a reference signal is maximum when the vibrissa angle $\theta(t) = \theta_{Ref}$; we identify the associated neuronal spike time as t_{Ref}. Similarly, the probability of an ON-contact signal is maximum when $\theta(t) = \theta_{ON}$, with associated spike time t_{ON}. We use these two constraints to eliminate the unknown phase ϕ from Equation 4 and obtain a relation for the contact angle. Near the center of the whisk cycle, this reduces to

$$\theta_{ON} \approx \theta_{Ref} + 2\pi \cdot \theta_0 f_{whisk} \cdot (t_{Ref} - t_{ON}), \qquad (6)$$

which shows that decoding of the contact angle depends on the difference in timing between reference- and contact-based spikes. We recall that reference signals, either from primary sensory or cortical neurons, span a range of preferred angles in the whisk cycle. In this population, there will always be reference neurons that spike close to the time of contact. The coincident detection of a contact spike and a reference spike for a neuron with preferred angle θ_{Ref} identifies the contact angle as $\theta_{ON} = \theta_{Ref}$. Similar solutions could be accomplished with ON- and OFF-contact signals or contact signals from separate vibrissae (Figure 2A), although these schemes involve increased complexity due to their inability to use coincidence.

Next Steps

The suggestion that mechanical resonances of the vibrissae contribute to neuronal encoding of surface texture is intriguing. An obvious test of this idea is to alter the vibrissae on an experienced rat to see if this impairs discrimination. Furthermore, there is a distinct lack of data on the nature of the transformation from high-frequency motion to firing rate. Electrophysiological recordings along the trigeminal-thalamocortical pathway are necessary to elucidate the nature of this code. Beyond texture discriminations, vibrations of the vibrissa may play a role in encoding contact with edges (Hartmann et al., 2003). The corresponding prediction is that contact will excite intrinsic vibrations and lead to a sensory spiking response that persists well beyond the time of contact.

While behavioral evidence for texture discrimination is strong, the corresponding evidence for object location is still developing. An essential missing experiment is to determine if rats can use their vibrissae to discriminate between similar objects positioned at different angles relative to the head. Assuming that rats succeed at this task, the question remains as to how reference and contact signals are combined. One scheme involves coincidence of spiking (Szwed et al., 2003). An alternative approach is based on the demodulation of rhythmically varying reference and contact signals (Ahrens et al., 2002; Szwed et al., 2003). Last, texture discrimination and object location may well be interrelated. Experimentally, this may be revealed if rats decode spatial variations in texture.

Selected Reading

Ahissar, E., Sosnik, R., and Haidarliu, S. (2000). Nature *406*, 302–306.

Ahrens, K.F., Levine, H., Suhl, H., and Kleinfeld, D. (2002). Proc. Natl. Acad. Sci. USA *99*, 15176–15181.

Arabzadeh, E., Petersen, R.S., and Diamond, M.E. (2003). J. Neurosci. *27*, 9146–9154.

Barth, D.S. (2003). J. Neurosci. *23*, 2502–2510.

Berg, R.W., and Kleinfeld, D. (2003). J. Neurophysiol. *89*, 104–117.

Brecht, M., Preilowski, B., and Merzenich, M.M. (1997). Behav. Brain Res. *84*, 81–97.

Carvell, G.E., and Simons, D.J. (1990). J. Neurosci. *10*, 2638–2648.

Carvell, G.E., and Simons, D.J. (1995). Somatosens. Mot. Res. *12*, 1–9.

Castro-Alamancos, M.A. (2002). J. Physiol. *539*, 567–578.

Cranch, E.T., and Adler, A.A. (1956). J. Appl. Mech. *78*, 103–108.

Deschenes, M., Timofeeva, E., and Lavallee, P. (2003). J. Neurosci. *23*, 6778–6787.

Engel, J., Schultens, H.A., and Schild, D. (1999). Biophys. J. *76*, 1310–1319.

Fee, M.S., Mitra, P.P., and Kleinfeld, D. (1997). J. Neurophysiol. *78*, 1144–1149.

Fend, M., and Bovet, S. Yokoi, H., and Pfeifer, R. (2003). IEEE/RSJ International Conference on Intelligent Robots and Systems (IROS), Las Vegas, NV, in press (www.amouse.de).

Gottschaldt, K.M., and Vahle-Hinz, C. (1981). Science *214*, 143–186.

Guic-Robles, E., Valdivieso, C., and Guajardo, G. (1989). Behav. Brain Res. *31*, 285–289.

Gustafson, J.W., and Felbain-Keramidas, S.L. (1977). Psychol. Bull. *84*, 477–488.

Hartmann, M.J., Johnson, N.J., Towal, R.B., and Assad, C. (2003). J. Neurosci. *23*, 6510–6519.

Harvey, M.A., Bermejo, R., and Zeigler, H.P. (2001). Somatosens. Mot. Res. *18*, 211–222.

Hutson, K.A., and Masterton, R.B. (1986). J. Neurophysiol. *56*, 1196–1223.

Krupa, D.J., Matell, M.S., Brisben, A.J., Oliveira, L.M., and Nicolelis, M.A.L. (2001). J. Neurosci. *21*, 5752–5763.

Neimark, M.A., Andermann, M.L., Hopfield, J.J., and Moore, C.I. (2003). J. Neurosci. *23*, 6499–6509.

Rice, F.L., Fundin, B.T., Pfaller, K., and Arvidsson, J. (1994). Exper. Brain Res. *99*, 233–246.

Schiffman, H.R., Lore, R., and Passafiume, J. (1970). Anim. Behav. *18*, 290–292.

Simons, D.J. (1978). J. Neurophysiol. *41*, 798–820.

Szwed, M., Bagdasarian, K., and Ahissar, E. (2003). Neuron *40*, 621–630.

Vincent, S.B. (1912). Behav. Mono. *1*, 7–81.

Zucker, E., and Welker, W.I. (1969). Brain Res. *12*, 134–156.